



A Fast Fault Location Based on a New Proposed Modern Metaheuristic Optimization Algorithm

Mohammad Parpaei¹, Hossein Askarian Abyaneh^{1*}, Farzad Razavi²

¹ Department of Electrical Engineering, Amirkabir University of Technology, Tehran, Iran

² Department of Electrical Engineering, Qazvin Branch, Islamic Azad University, Qazvin, Iran

ABSTRACT: Double-circuit power systems are one of the main types of modern transmission lines due to their reliability. Fault location in these transmission lines has always been a potential problem due to the mutual coupling between lines. Accordingly, this paper presents a novel objective function for the fault location using synchronous post-fault measurements of currents and voltages captured by distance protective relays. Moreover, a fast and accurate modern metaheuristic optimization algorithm for this cost function is proposed, which are key parameters to estimate the fault location methods based on optimization algorithms. In this regard, first, the input data (current and voltage signals) were refined using some auxiliary functions such as Fast Fourier transformation (FFT), Decaying Dc Elimination (DDE), and frequency tracking algorithm to accurately extract the fundamental component of the voltage and current signals. Afterwards, the proposed fault location based on the proposed metaheuristic optimization algorithm estimates the fault location using these input signals. The main advantage of the presented algorithm is the parallel estimation processing to improve the convergence speed and the accuracy of the objective function of the fault location, and was applied to various fault types and various operating conditions to validate the performance of the proposed approach. In addition, the performance of the proposed method was compared with different fault location methods. The simulation was implemented in the PSCAD and MATLAB® software. The simulation results show that the novel proposed approach outperforms other fault locations in estimating the fault location.

Review History:

Received: Jun. 16, 2022

Revised: Aug. 26, 2022

Accepted: Aug. 27, 2022

Available Online: Mar. 01, 2023

Keywords:

Fault Location

Power System

Transmission Line Fault Location

Optimization Algorithm

Distance Protective Relays

1- Introduction

In a power system, the faulty line section must be isolated in a sufficiently short amount of time after its inception. In this regard, protection relays have been utilized for identifying the location of faults, in addition to reliable event detection, and rapid system restoration. Hence, the Precise fault location algorithm is an important part of the protection schemes [1]. Different methods were proposed to exactly specify the fault location. In general, fault location methods can be divided into five categories. These fault locations may use the fundamental frequency of voltages and currents to use impedance-based methods, traveling wave theory, intelligent-based methods (or knowledge-based methods such as artificial intelligence techniques), high-frequency signals generated by faults, or wavelet transform-based methods.

A new approach based on the combination of the stability of the impedance-based method and the precision of the traveling waves was presented in [2]. An accurate one-terminal fault location algorithm based on the principle of short circuit calculation was presented by [3] and [4]. One of the most critical problems of the methods based on the one-terminal data was the fact that they are adversely affected

by the fault resistance. A new approach based on the voltage of both ends was addressed in [5] to eliminate the inherent error of the current transformer. Authors in [6] presented a new two-terminal numerical algorithm for fault location and arcing fault recognition. In order to employ the time-synchronized data of both ends of the power system, the authors in [7] proposed a new fault locator approach based on the Phasor Measurement Unit (PMU). A new method based on the time-synchronized data of the terminals in a double-circuit three-terminal transmission line was presented in [8]. This study uses PMUs to obtain simultaneous scattered measurements to formulate the fault location method. Due to the requirements of extensive communication links, the cost of commissioning is increased. A method based on the unsynchronized measurements on both sides was presented in [9-11]. Authors in [12-15] presented some methods based on the traveling wave. According to these methods, the fault inception and the arrival time of the traveling wave are used to estimate the fault location. A new method of calculating the speed of the earth mode component based on a single-ended traveling wave-based fault location algorithm was addressed in [16] to estimate the location of a fault. Authors in [17]

*Corresponding author's email: askarian@aut.ac.ir



Table 1. Shortcomings of the previous methods

Reference	Method Type	Shortcomings
[2]	Traveling wave	High-frequency data sampling
[3] and [4]	Impedance based	Sensitivity to the fault resistance
[5]	Impedance based	Single circuit power system
[6]	Impedance based	Single Phase to Ground
[9-11]	Impedance based	Single circuit power system
[12-18]	Traveling wave	High-frequency data sampling
[19]	Numerical algorithm	Single circuit power system
[20]	Optimization algorithm	Single circuit power system
[21, 22]	Intelligent-based	Implementing Difficulty

provide a method based on the time difference between the primary traveling wave and reflection. A new approach, including the accurate selection of faulty lines and a precise fault locator, was proposed in [18]. The main weakness of these methods is the need for high-frequency data sampling. A fault-location algorithm without utilizing line parameters based on the distributed line model was presented by [19]. In [20], a cost function to estimate fault location was proposed to reduce the simultaneous measurement errors. In [21, 22], a long short-term memory network was used to locate the fault in the network connected to wind turbines.

It should be noted that each of the existing fault locators has its own shortcomings, such as measurement errors, improper operation on two-circuit, sensitivity to the fault resistance, and high-frequency data sampling. Table 1 shows the shortcomings of the previous methods.

In this paper, a new objective function for the fault location of double-circuit power systems is presented. Moreover, a fast and accurate modern metaheuristic optimization algorithm for the function of the fault location estimation

on double-circuit power systems is proposed. The important characteristics, which must be carefully considered in the presented approaches, are speed and accuracy. In this regard, parallel processing is used to improve its speed. Moreover, to get sufficient estimation accuracy, a local search strategy is employed. The performance of the proposed intelligent optimization algorithm is compared to some other approaches, such as Eagle Strategy Coupled [23], Cuckoo Optimization Algorithm (COA)[24, 25], and Particle Swarm Optimization (PSO) [26-28]. Moreover, it was compared with the other kind of fault location methods presented in [29-31].

The rest of this paper is organized as follows. Section 2 discusses the proposed metaheuristic optimization algorithm. This optimization algorithm is tested with ten benchmark functions to address the accuracy and speed of the proposed optimization algorithm in Section 3, where a comparison is made with other conventional optimization algorithms. Section 4 presents the proposed fault location based on the Double-Circuit Power System. Results and discussions are presented in Section 5. Finally, the conclusions appear in Section 6.

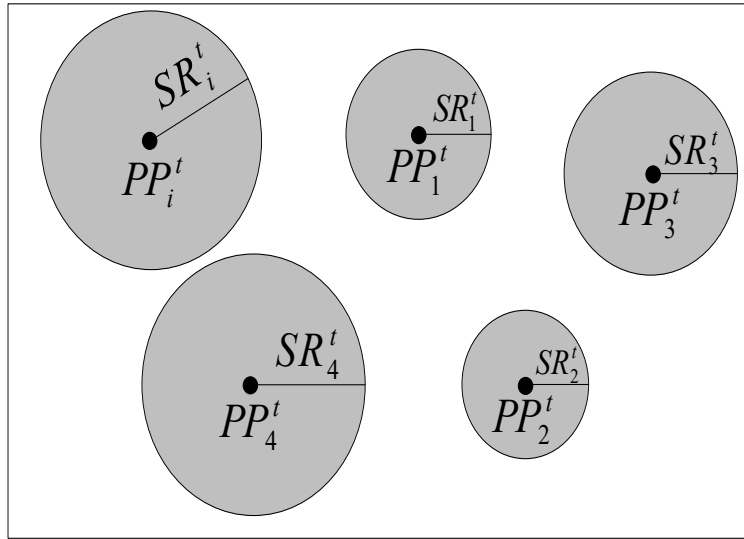


Fig. 1. Central points are the location of potential points

2- The Proposed Metaheuristic Optimization Algorithm

In this paper, a novel metaheuristic optimization algorithm is presented. The proposed approach is based on parallel search processing and an intensive local search strategy. This strategy contains four main stages that lead the optimization algorithm to the optimum point. These main stages are initializing, parallel and local search strategy, crossover, and convergence. Each step is completely described in the following sections.

2- 1- Initializing

The proposed optimization algorithm needs a vector to indicate initial points. This vector is defined as follows:

$$PP_i^t = (PP_{1,i}^t, PP_{2,i}^t, \dots, PP_{d,i}^t) \quad (1)$$

$\forall i \in \{1, 2, \dots, \text{parallel group size}\}$

where pp_i^t is i^{th} potential points that show the location of the i^{th} point in iteration, d is the dimension of the search space, and is the number of parallel processing in the search space. The stochastic initial points should be generated by the continuous probability distribution. Lévy distribution is a kind of distribution used to generate random numbers [26]. This distribution is as Eq. (2).

$$L(s) = \frac{1}{\pi} \int_0^\infty \cos(\tau s) e^{-\tau^\beta \alpha} d\tau \quad (2)$$

where is Lévy distribution, α and β are the constant factors. The special cases are $\beta = 1$ and $\beta = 2$ If β is equal to 1, Eq. (2) becomes the Cauchy distribution, and when β is equal to 2, Eq. (2) becomes a normal distribution. In this paper, it is considered that $\beta = 1$ and $\beta = 2$. Hence, the stochastic initial points will be generated by the normal distribution.

2- 2- Local Detection

In this stage, potential points keep searching the search space according to the Search Radius (SR) specified individually, as shown in Fig 1

In Fig 1, SR_i^t is the Search Radius of i^{th} potential point in iteration t . It should be noted that SR is different from points to point and is individually determined as Eq. (3).

$$SR_i^t = K \times \text{rand}(0,1) \times \frac{\text{var}_{\max}^t - \text{var}_{\min}^t}{\text{parallel group size}} \quad (3)$$

$\forall i \in \{1, 2, \dots, \text{parallel group size}\}$

where K is a positive number, and $\text{rand}(0,1)$ is a random number based on the distribution. var_{\min}^t and var_{\max}^t are minimum and maximum of variables, respectively.

The local search individually detects the best point in each circle. Therefore, a matrix that indicates the best local points should be made as Eq. (4).

$$BLP_i^t = [BLP_{1,i}^t, BLP_{2,i}^t, \dots, BLP_{d,i}^t], \quad (4)$$

$$\forall i \in \{1, 2, \dots, \text{group size}\}$$

where BLP_i^t is the best location point that i^{th} point (detected in its respective circle in iteration).

2- 3- Crossover

The crossover operator is an essential strategy to obtain the global maximum/minimum point of the objective function [32]. In this paper, a Stochastic Matrix () generated by a random number based on the normal distribution is used to make a Temporary Location () of the local points. Adaptive crossover probability, , controls the crossover operator by Eq. (5).

$$SM_i^t = (SM_{1,i}^t, SM_{2,i}^t, \dots, SM_{d,i}^t), \quad (5)$$

$$\forall i \in \{1, 2, \dots, \text{group size}\}$$

where SM_i^t is a matrix randomly generated, and Temporary Location (TL) of local points is given by:

$$TL_{i,j}^t = \begin{cases} SM_{i,j}^t & \text{rand}(0,1) > Cr \\ BLP_{i,j}^t & \text{otherwise} \end{cases}, \quad (6)$$

$$\forall i \in \{1, 2, \dots, \text{group size}\}, \forall j \in \{1, 2, \dots, d\}$$

where TL_i^t is a Temporary Location of the i^{th} local point, BLP_i^t is the best local point experienced by i^{th} potential point, $\text{rand}(0,1)$ is a random number based on the normal distribution, and is C_r the crossover probability and is defined as Eq. (7).

$$Cr = \frac{1}{a + \exp(-t)} \quad (7)$$

where a is a constant number and t is the iteration number. If the Temporary Location leads to a better solution, it will be replaced by the best local point as Eq. (8).

$$BLP_i^t = \begin{cases} TL_i^t & f(BLP_i^t) > f(TL_i^t) \\ BLP_i^t & \text{otherwise} \end{cases} \quad (8)$$

$$\forall i \in \{1, 2, \dots, \text{group size}\}$$

It is vital to note that Eq. (8) is for the cost function. If the objective function is a profit function, Eq. (9) should be used.

$$BLP_i^t = \begin{cases} TL_i^t & f(BLP_i^t) < f(TL_i^t) \\ BLP_i^t & \text{otherwise} \end{cases} \quad (9)$$

$$\forall i \in \{1, 2, \dots, \text{group size}\}$$

2- 4- Convergence

When local points detect the better point, other points move toward that location. The best point detected by the whole local points is selected as a global optimum point in the iteration, and other local points will converge to this point for the next iteration. Therefore, the best point is extracted from the best local point as a Global Point (GP) . Each of the points moves only a percentage of the total distance between the current local location and the global optimum location (since the optimization algorithm covers more points of search space). If it is assumed that the search space is d-dimensional space, the point location for the next iteration is a percentage of the total distance between the best local point and the Global Point in i^{th} dimension. Eq. (10) represents the convergence to the Global Point.

$$\begin{aligned} DP_{1,i}^{t+1} &= \text{rand}(0,1) \times (GP_1^t - BLP_{1,i}^t) + BLP_{1,i}^t \\ DP_{2,i}^{t+1} &= \text{rand}(0,1) \times (GP_2^t - BLP_{2,i}^t) + BLP_{2,i}^t \\ &\vdots \\ [DP_{d,i}^{t+1}] &= [\text{rand}(0,1) \times (GP_d^t - BLP_{d,i}^t) + BLP_{d,i}^t] \end{aligned} \quad (10)$$

$$\forall i \in \{1, 2, \dots, \text{group size}\}$$

where DP_i^{t+1} is an i^{th} local point in iteration $t + 1$, GP^t is the best point experienced by the whole local points in iteration t , BLP_i^t is the best local point experienced by the i^{th} point, and d is the dimension of search space.

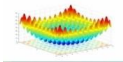
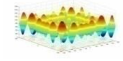
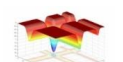
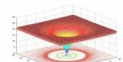
3- Validation of the Proposed Optimization Method

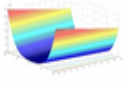
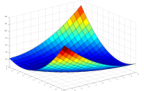
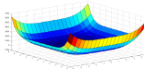
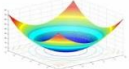
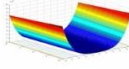
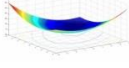
In this section, the proposed optimization, ES-DE, COA, and PSO have been applied to ten benchmark functions in order to confirm the superiority of the proposed optimization algorithm. The mean value (MEAN) and Standard Deviation (SD) are surveyed to validate the superiority of the proposed approach. The mean value states the average number of times that optimization algorithms obtain the global optimum point, and SD states the deviation from the mean value [33]. Table 2 presents the parameter values of the optimization algorithms. Different parameter values have been tested and then the best values are determined for each optimization method. Table 3 shows ten benchmark functions as touchstones [26, 32], and Table 4 provides simulation results of the proposed approach, ES-ED, COA, and PSO optimization algorithms. Function evaluations are carried out 10 times for all optimization algorithms.

Table 2. Parameter values of the optimization algorithms

Parameter values of the proposed algorithm		Parameter values of ES-DE	
Group size of the proposed approach	50	Stochastic population	50
K	0.4	F	0.5
a	1	C _r	0.5
Parameter values of COA		Parameter values of PSO	
Cuckoo population	50	Particle number	50
α	30	ω	0.95
		C ₁ , C ₂	2

Table 3. Details of benchmark functions used to validate the effectiveness of the proposed approach

Function name	Function equation	Domain	f _{min}	plot
Rastrigin	$f_1(X) = \sum_{i=1}^D (x_i^2 - 10\cos(2\pi x_i) + 10)$ $X = [x_1, x_2, \dots, x_D]$	$-5.12 < x_i < 5.12$	0	
Schwefel	$f_2(X) = 418.98287074 * D - \sum_{i=1}^D (x_i \sin \sqrt{ x_i })$ $X = [x_1, x_2, \dots, x_D]$	$-500 < x_i < 500$	0	
Michalewicz	$f_3(X) = - \sum_{i=1}^D (\sin(x_i) \times (\sin(\frac{ix_i^2}{\pi}))^{20})$ $X = [x_1, x_2, \dots, x_D]$	$0 < x_i < \pi$	**	
Ackley	$f_4(X) = -20 \exp \left(-0.2 \sqrt{D^{-1} \sum_{i=1}^D (x_i)^2} \right) - \exp \left(D^{-1} \sum_{i=1}^D \cos(2\pi x_i) \right) + 20 + \exp$ $X = [x_1, x_2, \dots, x_D]$	$-32 < x_i < 32$	0	

Rosenbrock	$f_5(X) = \sum_{i=1}^{D-1} (100(x_{i+1} - x_i^2)^2 + (x_i - 1)^2)$ $X = [x_1, x_2, \dots, x_D]$	$-30 < x_i < 30$	0	
Rotated hyper-ellipsoid	$f_6(X) = \sum_{i=1}^D \left(\sum_{j=1}^i x_j \right)^2$ $X = [x_1, x_2, \dots, x_D]$	$-100 < x_i, x_j < 100$	0	
Six-hump camel Back	$f_7(X) = 4x_1^2 - 2.1x_1^4 + \frac{x_1^6}{3} + x_1x_2 - 4x_2^2 + 4x_2^4$ $X = [x_1, x_2]$	$-5 < x_1, x_2 < 5$	-1.0	
sphere	$f_8(X) = \sum_{i=1}^D (x_i)^2$ $X = [x_1, x_2, \dots, x_D]$	$-100 < x_i < 100$	0	
Dixon & price	$f_9(X) = (x_1 - 1) + \sum_{i=1}^D i \times (2x_i^2 - x_{i-1})^2$ $X = [x_1, x_2, \dots, x_D]$	$-10 < x_i < 10$	0	
Trid	$f_{10}(X) = \sum_{i=1}^D (x_i - 1)^2 - \sum_{i=2}^D x_i x_{i-1}$ $X = [x_1, x_2, \dots, x_D]$	$-D^2 < x_1, \dots, x_D < D^2$	**	

**Different optimum points in different n-dimensional search spaces

Table 4. Numerical results of the proposed approach, ES, COA, and PSO for the benchmark functions

f_i	D	Proposed approach		ES-DE		COA		PSO	
		Mean	SD	Mean	SD	Mean	SD	Mean	SD
f_1	5	0	0	0	0	5.35783×1	1.15549×1	1.69452×1	3.39467×1
	10	7.68451×1	2.43005×1	1.96172×1	4.84012×1	3.30334×1	9.60925×1	6.84429	0.0012314
f_2	5	9.96540×1	2.39672×1	9.96542×1	1.24808×1	6.45879	1.39787×1	0.0164321	0.0248142
	10	1.00312×1	5.22354×1	1.99311×1	2.18336×1	0.0060318	0.0082025	0.0757905	0.1072248
f_3	5	-	9.36222×1	-	2.79009×1	-	0.0175566	-	1.66967×1
	10	-	0.0326959	-	0.0341040	-	0.0710060	-	0.0300132
f_4	5	3.01980×1	1.83461×1	8.88178×1	4.20431×1	4.36829×1	7.98149×1	4.78256×1	2.23768×1
	10	1.45595×1	2.91613×1	2.52825×1	8.49800×1	2.27095×1	3.84858×1	7.53328×1	2.56533×1
f_5	5	4.08993×1	1.07931×1	1.04836×1	2.28121×1	6.05139×1	1.00448×1	5.96790×1	1.23126×1
	10	7.15878×1	5.66244×1	8.69700×1	7.10552×1	9.87490×1	1.16593×1	3.34840	8.44309×1
f_6	5	5.21706×1	1.19139×1	4.44483×1	1.39268×1	3.19856	1.91520	2.08800×1	2.52435×1
	10	1.1412×10	2.35949×1	4.62754×1	7.63346×1	2.12772×1	5.96149×1	1.10839×1	1.19674×1
f_7	2	-	0	-	0	1.0316284	1.87162×1	-	6.68832×1
f_8	5	3.21491×1	8.40221×1	1.87212×1	1.47580×1	1.98761×1	6.42886×1	9.71316×1	5.84897×1
	10	4.94533×1	1.10471×1	1.46919×1	1.51440×1	1.16036×1	5.37851×1	1.61949×1	1.26256×1
f_9	5	3.79814×1	1.11734×1	3.66843×1	9.13407×1	9.23543×1	2.53906×1	5.22352×1	1.43824×1
	10	4.99171×1	4.29021×1	7.62888×1	5.80829×1	6.14653×1	5.10040×1	0.0101824	0.0082545
f_{10}	5	-	3.47065×1	-	9.62854×1	-	2.08851×1	-	0.0331214
	10	-	5.16312×1	-	0.0806672	-	1.2023193	-	4.3689537

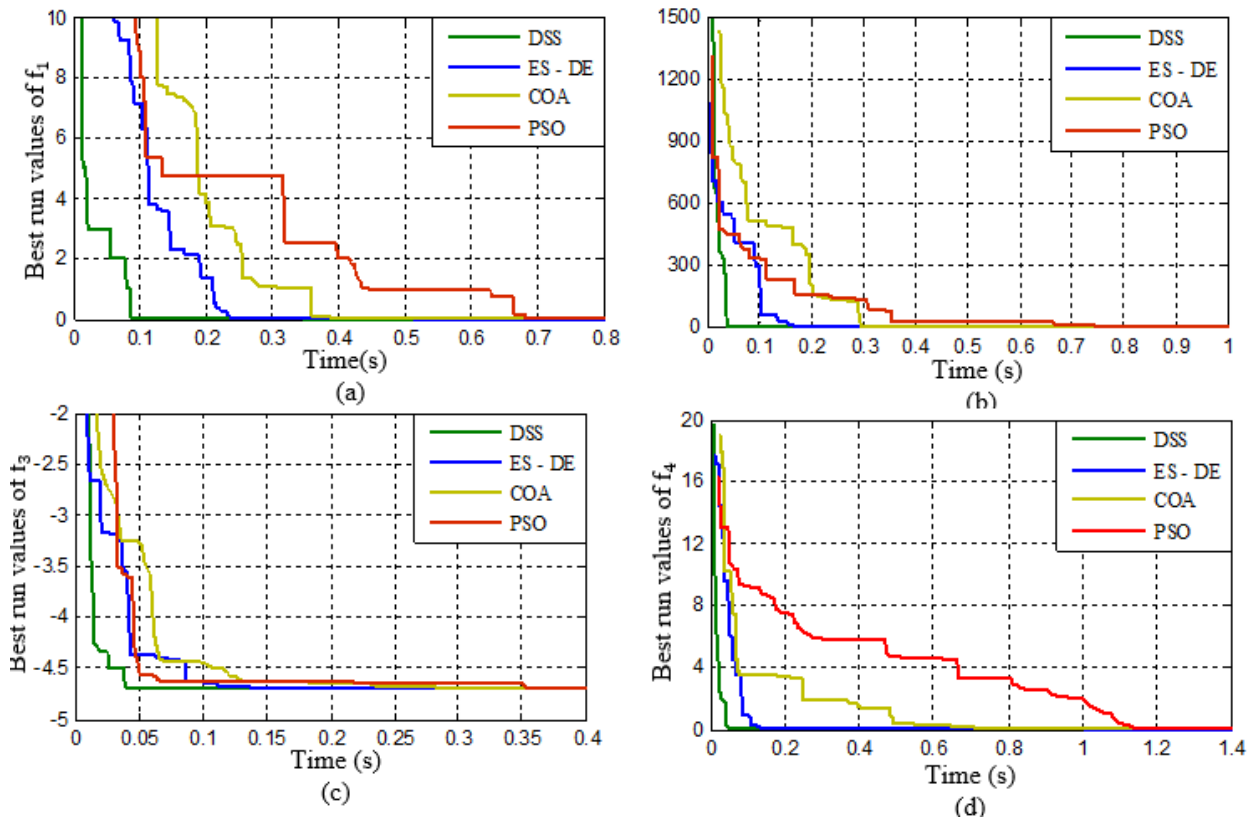


Fig. 2. Convergence characteristic of the proposed approach, ES- DE, COA, and PSO in best-run values of $f_1, f_2, f_3,$ and f_4 functions

The results in Table 4 confirm the performance of the proposed approach to ES-DE, COA, and PSO. Both Mean and SD parameters show the effectiveness of the proposed approach. It is obvious that the proposed approach outperforms ES-DE, COA, and PSO to detect the global optimum point of objective functions. In order to investigate the convergence speed of the proposed approach, ES-DE, COA, and PSO are applied to the $f_1, f_2, f_3,$ and f_4 functions that are multimodal. The outputs of the proposed optimization algorithm, ES-DE, COA, and PSO versus time are provided in Fig 2. As shown in this figure, the convergence speed of the proposed approach is higher than the other mentioned optimization algorithms.

4- The Proposed Fault Location Based on the Proposed Method in a Double-Circuit Power System

In the practical application, the frequency tracking and the Decaying Dc Elimination functions were applied to the current and voltage signals to modify the input data of the fault locator function [34, 35]. Generally, the expert system can be used for fault classification to select the fault type and its relative objective function, as shown in Fig 3.

In this section, a new objective function is presented to detect the fault location based on the information of the current

and voltage of the relay. The single line diagram of a double-circuit power system with a fault to the ground is shown in Fig 4. One of the biggest challenges facing the protective relay in this special type of power system is the mutual coupling between lines. Each parallel circuit, in addition to the self-impedance, experiences the mutual impedance generated by the other parallel circuit.

As shown in Fig 4, a single fault occurs in one of the circuits of the power system. The mutual coupling impedance between the two circuit lines is inversely related to the spacing between two lines. However, it is directly proportional to the length of the coupled section. In this regard, two parts of the coupled sections should be considered. Eq. (11) demonstrates the source impedance voltage drop, the voltage drop between relay location and fault point, fault impedance, and mutual impedance voltage drop.

$$V_S = Z_S * (I_{a|A} + I_{a|C}) + m * Z_{SR} * L * I_{a|C} + R_f * (I_{a|C} + I_{b|C} + I_{c|C} + I_{a|D} + I_{b|D} + I_{c|D}) + m * Z_m * (I_{a|A} + I_{b|A} + I_{c|A}) \quad (11)$$

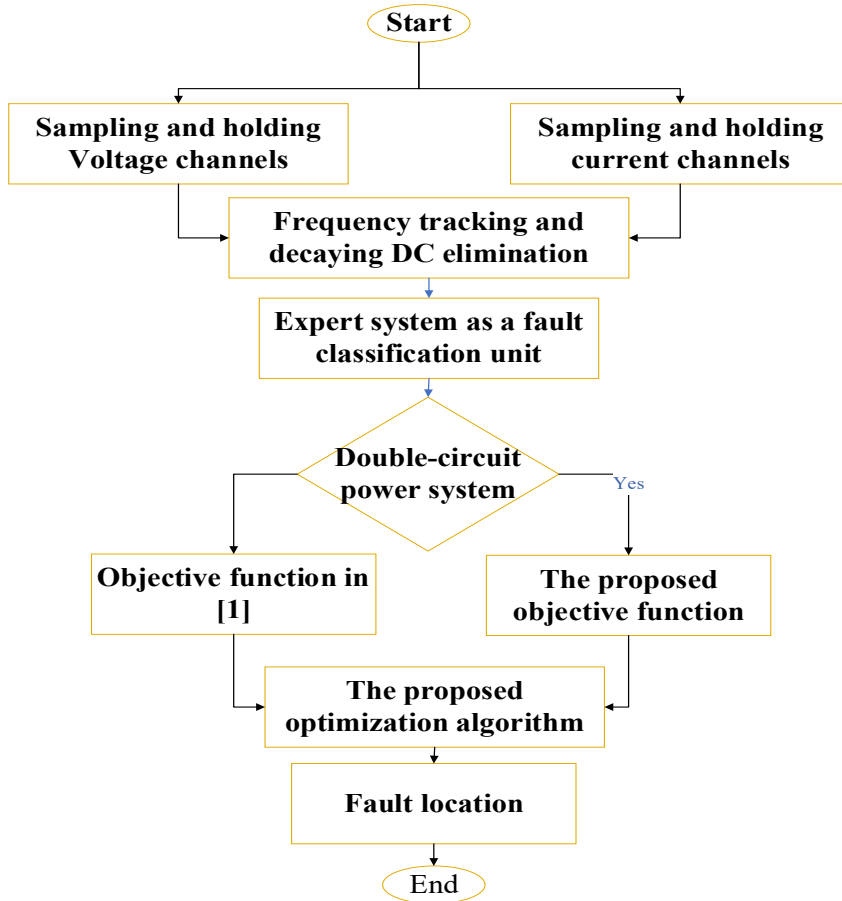


Fig. 3. the proposed fault location method

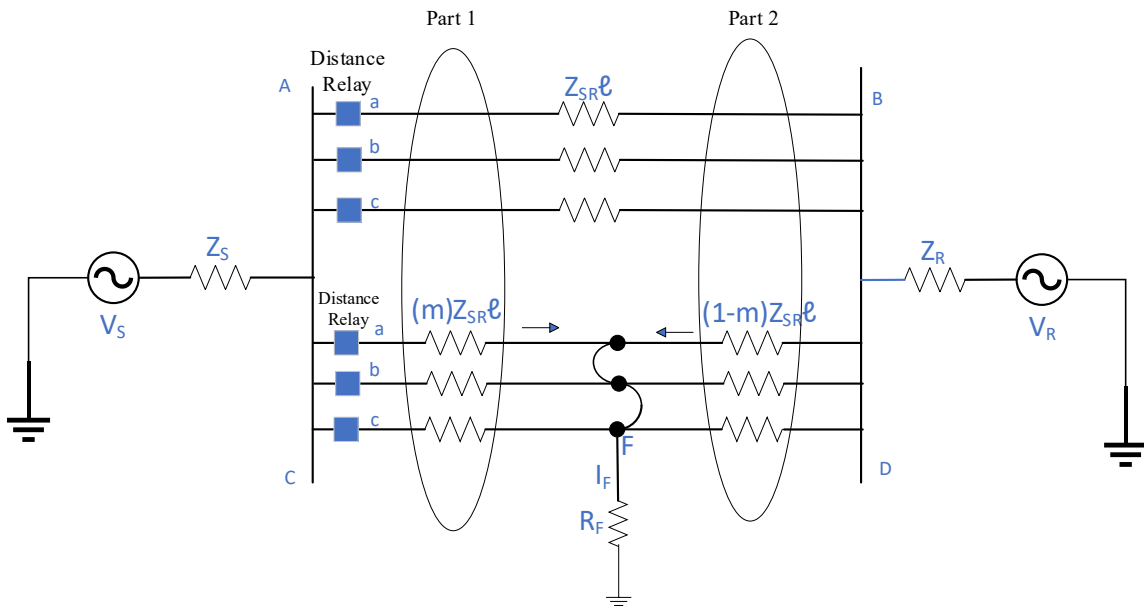


Fig. 4. Single line diagram of a two-circuit power system

where V_s is the voltage source, $(I_{a|c}, I_{b|c}, I_{c|c}), (I_{a|d}, I_{b|d}, I_{c|d}), (I_{a|A}, I_{b|A}, I_{c|A})$ are the three-phase current of “C”, “D”, and “A” sides of Fig 4, respectively. Z_s is source impedance, m is fault location, Z_{SR} is line impedance per kilometer, L is transmission line length, R_f is fault impedance, and Z_m is mutual coupling impedance.

Similar to Eq. (11), for the next loop (A to B path), Kirchhoff’s Voltage Law (KVL) is written as Eq. (12).

$$\begin{aligned}
 V_S = & Z_S * (I_{a|A} + I_{a|C}) + Z_{SR} * L * I_{a|A} + \\
 & (1 - m) * Z_{SR} * L * I_{a|D} + R_f * \\
 & (I_{a|C} + I_{b|C} + I_{c|C} + I_{a|D} + I_{b|D} + I_{c|D}) \\
 & + m * Z_m * (I_{a|C} + I_{b|C} + I_{c|C}) \\
 & - m * Z_m * (I_{a|D} + I_{b|D} + I_{c|D}) - \\
 & (1 - m) * Z_m * (I_{a|A} + I_{b|A} + I_{c|A})
 \end{aligned} \tag{12}$$

The parameters of Eq. (12) were described earlier. According to Eqs. (11) and (12), Eq. (13) can be obtained.

$$\begin{aligned}
 m * Z_{SR} * L * I_{a|C} + m * Z_m * (I_{a|A} + I_{b|A} + I_{c|A}) \\
 = Z_{SR} * L * I_{a|A} + (1 - m) * Z_{SR} * L * I_{a|D} + m * Z_m \\
 * (I_{a|C} + I_{b|C} + I_{c|C}) - m * Z_m * (I_{a|D} + I_{b|D} + I_{c|D}) \\
 - (1 - m) * Z_m * (I_{a|A} + I_{b|A} + I_{c|A})
 \end{aligned} \tag{13}$$

Eq. (13) can be sorted by $I_{a|D}$ as Eq. (14).

$$\begin{aligned}
 (1 - m) * Z_{SR} * L * I_{a|D} - m * \\
 Z_m * (I_{a|D} + I_{b|D} + I_{c|D}) \\
 = m * Z_{SR} * L * I_{a|C} + m * Z_m \\
 * (I_{a|A} + I_{b|A} + I_{c|A}) - Z_{SR} * L \\
 * I_{a|A} - m * Z_m * (I_{a|C} + I_{b|C} + I_{c|C}) \\
 + (1 - m) * Z_m * (I_{a|A} + I_{b|A} + I_{c|A})
 \end{aligned} \tag{14}$$

If the fault type is a phase-to-ground and the faulted phase is considered as phase a, Eq. (15) will be achieved.

$$\begin{aligned}
 I_{b|D} = -I_{b|C} \\
 I_{c|D} = -I_{c|C}
 \end{aligned} \tag{15}$$

On the other hand, Eq. (15) can be substituted in Eq. (14), yielding Eq. (16).

$$\begin{aligned}
 I_{b|D} = & \frac{-m * Z_m * (I_{b|C} + I_{c|C})}{(1 - m) * Z_{SR} * L - m * Z_m} + \\
 & \frac{+m * Z_{SR} * L * I_{a|C}}{(1 - m) * Z_{SR} * L - m * Z_m} - \\
 & \frac{-m * Z_m * (I_{a|C} + I_{b|C} + I_{c|C})}{(1 - m) * Z_{SR} * L - m * Z_m} + \\
 & \frac{m * Z_m * (I_{a|A} + I_{b|A} + I_{c|A})}{(1 - m) * Z_{SR} * L - m * Z_m} - \\
 & \frac{Z_{SR} * L * I_{a|A}}{(1 - m) * Z_{SR} * L - m * Z_m} + \\
 & \frac{(1 - m) * Z_m * (I_{a|A} + I_{b|A} + I_{c|A})}{(1 - m) * Z_{SR} * L - m * Z_m}
 \end{aligned} \tag{16}$$

The faulted current can be written as Eq. (17).

$$I_F = I_{a|C} + I_{b|C} + I_{c|C} + I_{a|D} + I_{b|D} + I_{c|D} \tag{17}$$

where I_F is the faulted current. The rest of the parameters were described earlier. According to Eq. (11), the faulted phase voltage can be written as Eq. (18).

$$\begin{aligned}
 V_F = R_f * (I_{a|C} + I_{b|C} + I_{c|C} + I_{a|D} + I_{b|D} + I_{c|D}) \\
 = V_S - Z_S * (I_{a|A} + I_{a|C}) + m * Z_{SR} * L * I_{a|C} + m * Z_m \\
 * (I_{a|A} + I_{b|A} + I_{c|A})
 \end{aligned} \tag{18}$$

where V_F is the faulted phase voltage. The relationship between the voltage and current angles in the fault point will be equal to Eq. (19).

$$\frac{\text{Imaginary}(I_F)}{\text{Real}(I_F)} = \frac{\text{Imaginary}(V_F)}{\text{Real}(V_F)} \tag{19}$$

where $\text{Imaginary}(I_F)$ and $\text{Imaginary}(V_F)$ are the imaginary parts of the current and the voltage of the fault point, respectively. $\text{Real}(I_F)$ and $\text{Real}(V_F)$ are the real

Table 5. Simulated Line Parameters

Parameter	Positive and negative sequence impedance	Zero-sequence impedance	
		self	mutual
Voltage Level	345 (kV)	self	mutual
Line Impedance	0.02+0.3j (Ω /km)	0.1458+0.8811j	0.1282+0.4610j
Source Impedance (S side)	0.25+7.4j (Ω)	1.7735+12.6286j	-
Source Impedance (R side)	0.21+5.15j(Ω)	0.4404+7.7961j	-
Line Length	60.314km	-	-

Table 6. Phase-to-ground fault results of the proposed approach

Fault Distance	Error (%)					
	Estimated fault location – Real fault location * 100					
	Real fault location					
	Zero Ω	0.5 Ω	5 Ω	50 Ω	100 Ω	150 Ω
10%	0.01	0.011	0.01	0.012	0.011	0.011
30%	0.01	0.018	0.024	0.03	0.04	0.037
50%	0.03	0.034	0.04	0.039	0.048	0.052
70%	0.04	0.049	0.052	0.06	0.055	0.064
90%	0.05	0.056	0.057	0.055	0.055	0.056

parts of the current and the voltage of the fault point, respectively. Eq. (19) can be rewritten as an objective function for the optimization algorithm using Eq. (20)

Objective Function =

$$\left| \frac{\text{Imaginary}(I_F)}{\text{Real}(I_F)} - \frac{\text{Imaginary}(V_F)}{\text{Real}(V_F)} \right| \quad (20)$$

According to Fig 4, it should be noted that the current and voltage data of the “A” and “C” sides of the power system are captured by the protective relay, and fault location is estimated by the proposed optimization algorithm.

5- Results and Discussions

The parameter values of the studied system are given in Table 5. In order to validate the performance of the proposed algorithm, the power system illustrated in Fig 4 is simulated in the PSCAD software. The current and voltage of the distance relay will be captured as a Comtrade file and used by the proposed fault location function simulated in MATLAB software. In this regard, different fault conditions are implemented to evaluate the accuracy and speed of the proposed approach.

Among the various fault types, the phase-to-ground fault is one of the most possible faults in the power system. Moreover, the fault impedance in double-circuit lines is also another serious challenge due to the mutual impedance. To evaluate the performance of the proposed approach, different

Table 7. three-phase fault results of the proposed approach

Fault Distance	Error (%)					
	$\frac{ \text{Estimated fault location} - \text{Real fault location} }{\text{Real fault location}} * 100$					
	Zero Ω	0.5 Ω	5 Ω	50 Ω	100 Ω	150 Ω
10%	0.01	0.01	0.01	0.01	0.012	0.011
30%	0.01	0.01	0.012	0.01	0.012	0.013
50%	0.015	0.015	0.012	0.015	0.011	0.011
70%	0.018	0.020	0.019	0.017	0.017	0.020
90%	0.02	0.017	0.018	0.02	0.02	0.019

Table 8. Comparison of the proposed method with other fault location methods

Reference	Error
	$\frac{ \text{Estimated fault location} - \text{Real fault location} }{\text{Real fault location}} * 100$
[29]	8.15
[30]	1.29
[31]	8.06
Proposed method	0.052

fault distances with a phase-to-ground fault are implemented with an interval of 20%. One of the main factors in the investigation of fault location algorithms is fault impedance sensitivity. In order to consider this factor, fault impedance has been changed from 0 to 150 Ω . The simulation results are shown in Table 6.

To address the performance of the proposed algorithm in a three-phase fault type, this fault type is applied to the simulated power system. Table 7 shows the results of the proposed method.

In order to confirm the superiority of the proposed fault location, Table 8 provides a comparison with the other fault location approaches in terms of performance accuracy.

As can be seen from Table 8, the error value of the proposed method is much smaller than other fault location methods, and it operates more precisely. Moreover, in order to compare the proposed approach with other optimization algorithms, such as PSO and COA, these methods have been applied to the same power system when the fault occurs at 0.2 of transmission line length from the 'C' side with the fault resistance of 10 (Ω). Fig 5 shows the execution time of simulation results.

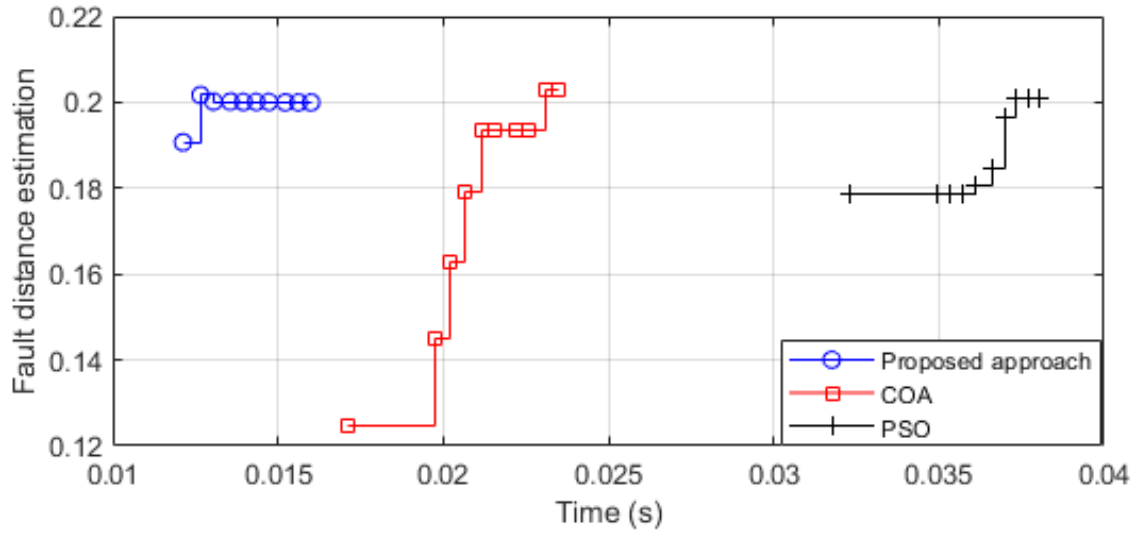


Fig. 5. Execution time analysis of the proposed approach, PSO, and COA in the same situation (the fault resistance is 10 (Ω) and the fault distance from sending end is 0.2)

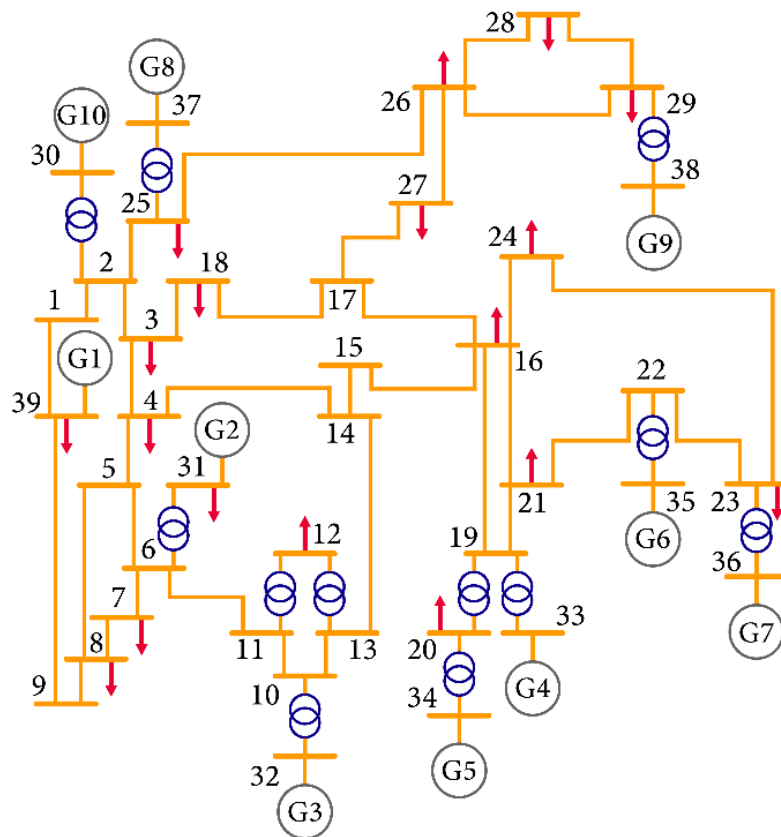


Fig. 6. IEEE 39-bus system

Table 9. Different three phases fault type scenarios

Fault Location	Fault Type	Fault Distance	Error (%)			Execution time (seconds)
			Estimated fault location – Real fault location			
			Real fault location			0.010
			Zero Ω	5 Ω	50 Ω	
Line 25-26	ABCG*	10%	0.01	0.01	0.02	0.012
Line15-16	ABCG	50%	0.013	0.015	0.016	0.011
Line15-16	ABCG*	80%	0.017	0.02	0.022	0.013
Line15-16	AG*	50%	0.029	0.041	0.042	0.014

* ABCG= Three Phases to the ground fault type

AG*= Phase A to the ground fsault type

In order to further investigation, the proposed method was tested in the IEEE 39-bus system (Fig 6), in which detailed generator model and constant impedance loads are taken into account [36]. Table 9 shows the simulation results of the proposed method in different fault resistances and different fault locations.

6- Conclusion

In this paper, the novel strategy based on the parallel processing and local search strategy is presented. Due to the adaptive crossover and local search of the proposed approach, it can detect the Global Point of objective functions with higher accuracy and convergence speed than conventional methods, such as COA, ES-DE, and PSO. In addition, a new intelligent fault location approach for a double-circuit power system is presented. The main advantage is the simple structure (without the presence of any tedious mathematical equations) that begets a higher speed than the conventional approach to detecting the fault location. The other advantage of the proposed fault location is its impassibility to fault resistance. Both the novel optimization algorithm and the proposed intelligent fault location approach are superior to the conventional approaches.

References

- [1] N. Ghaffarzadeh, M. Parpaei, and M. Z. Tayar, "A fast fault location method based on detecting the minimum number of Phasor Measurement Units using a novel adaptive binary differential evolution optimization algorithm," *International Transactions on Electrical Energy Systems*, vol. 25, no. 11, pp. 2933-2947, 2015.
- [2] B. Wang, X. Dong, L. Lan, and F. Xu, "Novel location algorithm for single-line-to-ground faults in transmission line with distributed parameters," *IET Generation, Transmission & Distribution*, vol. 7, no. 6, pp. 560-566, 2013.
- [3] W. Threevithayanon and N. Hoonchareon, "Accurate one-terminal fault location algorithm based on the principle of short-circuit calculation," *IEEJ transactions on electrical and electronic engineering*, vol. 8, no. 1, pp. 28-32, 2013.
- [4] Z. M. Radojevic and J.-R. Shin, "New one terminal digital algorithm for adaptive reclosing and fault distance calculation on transmission lines," *IEEE Transactions on Power Delivery*, vol. 21, no. 3, pp. 1231-1237, 2006.
- [5] S. M. Brahma and A. A. Girgis, "Fault location on a transmission line using synchronized voltage measurements," *IEEE Transactions on power Delivery*, vol. 19, no. 4, pp. 1619-1622, 2004.
- [6] C. Lee, J. Park, J. Shin, and Z. Radojevie, "A new two-terminal numerical algorithm for fault location, distance protection, and arcing fault recognition," *IEEE Transactions on Power Systems*, vol. 21, no. 3, pp. 1460-1462, 2006.
- [7] M. Parpaei, N. Ghaffarzadeh, and M. Z. Tayar, "Rational random walk-based optimal placement of

- Phasor Measurement Units to enhance the initializing and guiding the optimization processes,” *International Transactions on Electrical Energy Systems*, vol. 27, no. 7, p. e2323, 2017.
- [8] V. K. Gaur and B. Bhalja, “New fault detection and localisation technique for double-circuit three-terminal transmission line,” *IET Generation, Transmission & Distribution*, vol. 12, no. 8, pp. 1687-1696, 2018.
- [9] C.-S. Yu, L.-R. Chang, and J.-R. Cho, “New fault impedance computations for unsynchronized two-terminal fault-location computations,” *IEEE transactions on power delivery*, vol. 26, no. 4, pp. 2879-2881, 2011.
- [10] S. Hussain and A. Osman, “Fault location scheme for multi-terminal transmission lines using unsynchronized measurements,” *International Journal of Electrical Power & Energy Systems*, vol. 78, pp. 277-284, 2016.
- [11] M. A. Elsadd and A. Y. Abdelaziz, “Unsynchronized fault-location technique for two-and three-terminal transmission lines,” *Electric Power Systems Research*, vol. 158, pp. 228-239, 2018.
- [12] P. Gale, P. Taylor, P. Naidoo, C. Hitchin, and D. Clowes, “Travelling wave fault locator experience on Eskom’s transmission network,” 2001.
- [13] P. McLaren and S. Rajendra, “Travelling-wave techniques applied to the protection of teed circuits:-multi-phase/multi-circuit system,” *IEEE Transactions on Power Apparatus and Systems*, no. 12, pp. 3551-3557, 1985.
- [14] C. Y. Evrenosoglu and A. Abur, “Travelling wave based fault location for teed circuits,” *IEEE Transactions on Power Delivery*, vol. 20, no. 2, pp. 1115-1121, 2005.
- [15] A. Sharafi, M. Sanaye-Pasand, and P. Jafarian, “Ultra-high-speed protection of parallel transmission lines using current travelling waves,” *IET Generation, Transmission & Distribution*, vol. 5, no. 6, pp. 656-666, 2011.
- [16] R. Benato, S. D. Sessa, M. Poli, C. Quaciari, and G. Rinzo, “An online travelling wave fault location method for unearthed-operated high-voltage overhead line grids,” *IEEE Transactions on Power Delivery*, vol. 33, no. 6, pp. 2776-2785, 2018.
- [17] F. Xu and X. Dong, “A novel single-ended traveling wave fault location method based on reflected wave-head of adjacent bus,” 2014.
- [18] Z. Li, Y. Cheng, X. Wang, Z. Li, and H. Weng, “Study on wide-area traveling wave fault line selection and fault location algorithm,” *International Transactions on Electrical Energy Systems*, vol. 28, no. 12, p. e2632, 2018.
- [19] Y. Liao and N. Kang, “Fault-location algorithms without utilizing line parameters based on the distributed parameter line model,” *IEEE Transactions on Power Delivery*, vol. 24, no. 2, pp. 579-584, 2009.
- [20] Y. Liao and M. Kezunovic, “Optimal estimate of transmission line fault location considering measurement errors,” *IEEE Transactions on Power Delivery*, vol. 22, no. 3, pp. 1335-1341, 2007.
- [21] B. Taheri, S. Salehimehr, and M. Sedighizadeh, “A fault-location algorithm for parallel line based on the long short-term memory model using the distributed parameter line model,” *International Transactions on Electrical Energy Systems*, vol. 31, no. 11, p. e13032, 2021.
- [22] B. Taheri, S. Salehimehr, and M. Sedighizadeh, “A novel strategy for fault location in shunt-compensated double circuit transmission lines equipped by wind farms based on long short-term memory,” *Cleaner Engineering and Technology*, p. 100406, 2022.
- [23] A. H. Gandomi, X.-S. Yang, S. Talatahari, and S. Deb, “Coupled eagle strategy and differential evolution for unconstrained and constrained global optimization,” *Computers & Mathematics with Applications*, vol. 63, no. 1, pp. 191-200, 2012.
- [24] R. Rajabioun, “Cuckoo Optimization Algorithm,” *Applied soft computing*, vol. 11, no. 8, pp. 5508-5518, 2011.
- [25] M. Dosararian-Moghadam and Z. Amo-Rahimi, “Energy Efficiency and Reliability in Underwater Wireless Sensor Networks Using Cuckoo Optimizer Algorithm,” *AUT Journal of Electrical Engineering*, vol. 50, no. 1, pp. 93-100, 2018, doi: 10.22060/ej.2018.13347.5154.
- [26] R. N. Mantegna and H. E. Stanley, “Stochastic process with ultraslow convergence to a Gaussian: the truncated Lévy flight,” *Physical Review Letters*, vol. 73, no. 22, p. 2946, 1994.
- [27] H. Rezagholizadeh and D. Gharavian, “A Thinning Method of Linear And Planar Array Antennas To Reduce SLL of Radiation Pattern By GWO And ICA Algorithms,” *AUT Journal of Electrical Engineering*, vol. 50, no. 2, pp. 135-140, 2018, doi: 10.22060/ej.2018.13697.5182.
- [28] B. Farhadi, S. H. Shahalami, and E. Fallah Choolabi, “Optimal Design of Single-Phase Induction Motor Using MPSO and FEM,” *AUT Journal of Electrical Engineering*, vol. 46, no. 1, pp. 1-9, 2014, doi: 10.22060/ej.2014.435.
- [29] M.-S. Choi, S.-J. Lee, D.-S. Lee, and B.-G. Jin, “A new fault location algorithm using direct circuit analysis for distribution systems,” *IEEE transactions on power delivery*, vol. 19, no. 1, pp. 35-41, 2004.
- [30] R. Salim, K. Salim, and A. Bretas, “Further improvements on impedance-based fault location for power distribution systems,” *IET Generation, Transmission & Distribution*, vol. 5, no. 4, pp. 467-478, 2011.
- [31] R. H. Salim, M. Resener, A. D. Filomena, K. R. C. De Oliveira, and A. S. Bretas, “Extended fault-location formulation for power distribution systems,” *IEEE transactions on power delivery*, vol. 24, no. 2, pp. 508-516, 2009.
- [32] A. H. Gandomi and A. H. Alavi, “Krill herd: a new bio-

- inspired optimization algorithm,” *Communications in nonlinear science and numerical simulation*, vol. 17, no. 12, pp. 4831-4845, 2012.
- [33] R. Azizipanah-Abarghooee, “A new hybrid bacterial foraging and simplified swarm optimization algorithm for practical optimal dynamic load dispatch,” *International Journal of Electrical Power & Energy Systems*, vol. 49, pp. 414-429, 2013.
- [34] S. S. K. Madahi, H. A. Abyaneh, C. A. Nucci, and M. Parpaei, “A new DFT-based frequency estimation algorithm for protection devices under normal and fault conditions,” *International Journal of Electrical Power & Energy Systems*, vol. 142, p. 108276, 2022.
- [35] M. Parpaei, H. A. Abyaneh, and F. Razavi, “An innovative method to eliminate multiple exponentially decaying DC components based on the discrete Fourier transform in the numerical distance relay,” *IET Generation, Transmission & Distribution*, 2022.
- [36] F. Fallahi and P. Naderi, “Analyzing the internal resonances and energy exchange between modes of power system considering Frequency – Energy dependence using Pseudo-Arclength and shooting algorithm,” *AUT Journal of Electrical Engineering*, vol. 52, no. 1, pp. 53-62, 2020, doi: 10.22060/ej.2020.17351.5310.

HOW TO CITE THIS ARTICLE

M. Parpaei, H. Askarian Abyaneh, F Razavi, A Fast Fault Location Based on a New Proposed Modern Metaheuristic Optimization Algorithm, AUT J Electr Eng, 55(1) (2023) 31-46.

DOI: [10.22060/ej.2022.21498.5477](https://doi.org/10.22060/ej.2022.21498.5477)

